

KAN-AFT: An Interpretable Nonlinear Survival Model Integrating Kolmogorov-Arnold Networks with Accelerated Failure Time Analysis

Mebin Jose^a, Jisha Francis^{a,*}, Sudheesh Kumar Kattumannil^b

^a*Department of Mathematics, School of Advanced Sciences,
Vellore Institute of Technology, Vellore, India, 632014.*

^b*Applied Statistics Unit, Indian Statistical Institute, Chennai, India, 600029.*

Abstract

Survival analysis relies fundamentally on the semi-parametric Cox Proportional Hazards (CoxPH) model and the parametric Accelerated Failure Time (AFT) model. CoxPH assumes constant hazard ratios, often failing to capture real-world dynamics, while traditional AFT models are limited by rigid distributional assumptions. Although deep learning models like DeepAFT address these constraints by improving predictive accuracy and handling censoring, they inherit the significant challenge of black-box interpretability. The recent introduction of CoxKAN demonstrated the successful integration of Kolmogorov-Arnold Networks (KANs), a novel architecture that yields highly accurate and interpretable symbolic representations, within the CoxPH framework. Motivated by the interpretability gains of CoxKAN, we introduce KAN-AFT (Kolmogorov Arnold Network-based AFT), the first framework to apply KANs to the AFT model. KAN-AFT effectively models complex non-linear relationships within the AFT framework. Our primary contributions include: (i) a principled AFT-KAN formulation, (ii) robust optimization strategies for right-censored observations (e.g., Buckley-James and IPCW), and (iii) an interpretability pipeline that converts the learned spline functions into closed-form symbolic equations for survival time. Empirical results on multiple datasets confirm that KAN-AFT achieves performance comparable to or better than DeepAFT, while uniquely providing transparent, symbolic models of the survival process.

Keywords: Accelerated Failure Time (AFT) model, Kolmogorov-Arnold Networks

*Corresponding author: Jisha Francis, Email: jishafrancis@vit.ac.in

1. Introduction

Survival analysis is a specialized field concerned with modeling and analyzing the time until the occurrence of a specific event of interest, often referred to as time-to-event or failure-time data (Wang et al., 2019). A defining characteristic of survival data is the presence of censoring, where the precise event time is unknown, but partial information (e.g., the event did not occur by the last observation time) is available. Handling these censored observations is crucial, as traditional regression methods yield biased results (Norman et al., 2024).

Censoring typically arises in longitudinal (data collected from the same subjects repeatedly over time) or clinical studies when some individuals do not experience the event during the observation period. For example, a patient in a clinical trial may withdraw before completion, or the study may end before disease recurrence occurs. In these cases, it is only known that the event did not occur up to a certain time point, while the exact time of occurrence remains unobserved (Buckley and James, 1979; Fan and Gijbels, 1994).

The primary objective of survival analysis is to determine how explanatory variables (covariates) which may include patient characteristics, treatment types, or environmental factors affect the time to an event. These covariates are typically incorporated into regression-based survival models to estimate risk or predict the median survival time. Standard regression techniques, such as linear regression, are not suitable for this purpose because they cannot properly handle censored data and thus produce biased results (Klein and Moeschberger, 2003). To address this problem, specialized survival models have been developed. Two foundational statistical models have historically dominated this field: the Cox Proportional Hazards (CoxPH) model and the Accelerated Failure Time (AFT) model.

The CoxPH model (Cox, 1972) is a semi-parametric model that represents the instantaneous risk (hazard) for an individual as a proportion of a baseline hazard function $h_0(t)$, defined as:

$$h_i(t|\mathbf{x}_i) = h_0(t) \exp(\mathbf{x}_i^\top \boldsymbol{\beta}), \quad t > 0,$$

where $\mathbf{x}_i^\top \boldsymbol{\beta}$ is the linear predictor. The corresponding survival function, $S(t|\mathbf{x}_i)$, is derived

from the cumulative hazard, $H(t | x_i) = \int_0^t h(u | x_i) du$, resulting in a multiplicative scaling of the baseline survival:

$$S(t | \mathbf{x}_i) = [S_0(t)]^{\exp(\mathbf{x}_i^\top \boldsymbol{\beta})}, \quad t > 0,$$

where $S_0(t)$ is the baseline survival function. The strength of the CoxPH model lies in its flexibility, as it avoids strict assumptions about the shape of the baseline hazard. However, its core weakness is the strict reliance on the Proportional Hazards assumption, which dictates that the hazard ratio $\exp(\mathbf{x}_i^\top \boldsymbol{\beta})$ remains constant over time. This assumption is often violated in practical applications (Knottenbelt et al., 2025).

Turning the focus to the AFT model (Wei, 1992), we observe that it offers a more direct, time-based interpretation by modeling the logarithm of the survival time T_i as a log-linear function of the covariates. The full log-linear representation for an individual i is given by:

$$\log T_i = \mu + \beta_1 z_{i1} + \beta_2 z_{i2} + \cdots + \beta_p z_{ip} + \sigma \epsilon_i, \quad i = 1, 2, \dots, n \quad (1)$$

where z_{i1}, \dots, z_{ip} are the p explanatory variables, β_j are their coefficients, μ is the intercept, σ is the scale parameter, and ϵ_i is the standardized error term following a specified distribution. To express this relationship in a matrix-vector product, the equation is written in compact form as:

$$\log(T_i) = \mathbf{x}_i^\top \boldsymbol{\beta} + \sigma \epsilon_i, \quad (2)$$

where the augmented covariate vector \mathbf{x}_i is formed by appending the constant 1 to the beginning of the feature vector, $\mathbf{z}_i = (z_{i1}, \dots, z_{ip})^\top$, such that $\mathbf{x}_i = (1, z_{i1}, \dots, z_{ip})^\top$. Consequently, the coefficient vector $\boldsymbol{\beta}$ is also augmented to include the intercept: $\boldsymbol{\beta} = (\mu, \beta_1, \dots, \beta_p)^\top$. This formulation enables accurate maximum likelihood estimation. The survival function of the AFT model clearly defines its characteristic time-scaling property:

$$S(t | \mathbf{x}) = S_0 \left(t \cdot \exp(-\mathbf{x}^\top \boldsymbol{\beta}) \right).$$

The core of the AFT model's time-scaling property is the acceleration factor, defined as $\exp(\mathbf{x}^\top \boldsymbol{\beta})$, which directly quantifies how covariates stretch or compress the expected time to an event relative to a baseline. If this factor is greater than 1, it signifies time dilation

(e.g., a factor of 1.5 increases expected survival by 50%), meaning the event is delayed; conversely, a factor less than 1 indicates time compression, meaning the event occurs sooner. The model's incorporation of the negative exponent ($-\mathbf{x}^\top \boldsymbol{\beta}$) ensures that the coefficient signs align directly with their effect on time: a positive coefficient ($\beta_j > 0$) corresponds to an acceleration factor > 1 (desirable time dilation), while a negative coefficient ($\beta_j < 0$) corresponds to a factor < 1 (undesirable time compression). This direct, time-based interpretation is inherently intuitive and highly practical, offering a transparent measure of covariate influence without relying on the complexity of hazard ratio interpretation or the strict Proportional Hazards assumption.

From the above discussion, it is evident that the AFT model provides a more accurate and robust alternative when the common Proportional Hazards (PH) assumption is violated, meaning that covariate effects vary over time (Wei, 1992; Lee and Wang, 2003). Furthermore, the AFT framework is particularly effective when survival time itself is the primary outcome, as often occurs in fields such as aging research or clinical trials focused on lifespan or time to recovery. In these cases, the time-scaling interpretation of the AFT model makes it easy to understand and explain how factors affect survival time, showing whether they speed it up (accelerating) or slow it down (Hutton and Monaghan, 2002; Swindell, 2009). Lastly, provided that suitable parametric assumptions are utilized, the AFT approach remains a powerful and efficient modeling choice for analyzing heavily censored data or data collected from small samples (Lee and Wang, 2003).

Despite these strengths, traditional AFT models are constrained by the need to specify an appropriate parametric distribution for ϵ_i and their reliance on linear predictors, which limit the capacity to capture complex, nonlinear covariate relationships (Norman et al., 2024). The first constraint presents a practical challenge, as the correct distribution (e.g., Weibull, log-normal, or generalized gamma) must be selected based on the underlying data, and misspecification can lead to biased coefficient estimates and inaccurate predictions. More significantly, the assumption of a linear relationship between the log-transformed survival time and the covariates often oversimplifies complex biological, clinical, or economic systems where covariate interactions and non-additive effects are prevalent.

To overcome these inherent limitations and enhance model flexibility, the past decade

has witnessed a significant shift toward Machine Learning (ML) and Deep Learning (DL) approaches in survival analysis. Early ML methods, such as Random Survival Forests (Ishwaran et al., 2008) and Gradient Boosting Machines (Chen et al., 2013), introduced nonparametric and highly flexible frameworks capable of capturing complex covariate interactions without requiring specific distributional assumptions. Faraggi and Simon (1995) introduced the nonlinear ANN predictor in the area of survival analysis by extending the Cox PH model to fit a neural network with a linear output layer and a single logistic hidden layer. DL models leverage Deep Neural Networks (DNNs) to automatically learn complex, high-dimensional feature representations. Early DL methods often extended the Cox Proportional Hazards framework, such as DeepSurv (Katzman et al., 2018) and DeepHit (Lee et al., 2018), which introduced time-dependent predictions and competitive risk modeling. More recently, the Deep Accelerated Failure Time (DeepAFT) model (Norman et al., 2024) successfully integrated DNNs into the AFT model by replacing the rigid linear predictor with a non-linear network $\eta(\mathbf{x}_i)$. This allows DeepAFT to overcome the rigid distributional and linear assumptions of classical AFT models while incorporating robust strategies to handle right-censoring, such as the Buckley-James imputation method and Inverse Probability Censoring Weights (IPCW) (Norman et al., 2024).

Despite their superior predictive performance, ML and DL models in survival analysis are often limited by their black-box nature (Knottenbelt et al., 2025). In high-stakes fields like medicine and finance, this lack of transparency (the inability to provide a clear rationale behind predicted survival times) limits clinical adoption, driving active research into Interpretable Machine Learning (IML) techniques (Xu and Guo, 2023).

Kolmogorov-Arnold Networks (KANs) (Liu et al., 2024) have recently emerged as an alternative to Multi-Layer Perceptrons (MLPs), demonstrating superior accuracy and enhanced interpretability. Unlike MLPs, KANs place learnable activation functions, parameterized by splines, on the edges of the network (Somvanshi et al., 2025). This unique architecture allows the final function approximation to be converted into a concise, closed-form symbolic formula (Knottenbelt et al., 2025). The potential of KANs in survival analysis was recently demonstrated by CoxKAN (Knottenbelt et al., 2025), which achieved symbolic representations of the hazard function while outperforming standard CoxPH and matching

DeepSurv.

In this work, we introduce KAN-AFT, the first framework to integrate the KAN architecture within the AFT model. By combining the natural time-based interpretation of the AFT model with the symbolic interpretability of KANs, KAN-AFT offers a uniquely powerful, transparent, and high-performance approach to survival analysis. Furthermore, this study develops KAN-AFT to enhance both interpretability and predictive accuracy while effectively handling right-censored survival data. To address censoring, we incorporate three established approaches inspired by the DeepAFT model (Norman et al., 2024): (i) iterative imputation of right-censored observations to estimate complex nonlinear functions (Buckley and James, 1979), (ii) the use of inverse probability of censoring weights (IPCW) (Robins and Rotnitzky, 1992), and (iii) the transformation method proposed by Fan and Gijbels (Fan et al., 1997).

The detailed formulation of the proposed KAN-AFT model is presented in Section 2, followed by experimental evaluation and comparative results in Section 3 with simulation studies. The real life applications of KAN-AFT is discussed in Section 4 with four real data sets, Mayo Clinic Primary Biliary Cholangitis (PBC) data, German Breast Cancer Study Group (GBSG) data, Veteran data and Heart failure clinical data. Section 5 concludes, the paper with discussions and future directions.

2. Kolmogorov-Arnold Network for AFT (KAN-AFT)

The Accelerated Failure Time (AFT) model proved as a powerful framework in survival analysis that directly regresses the logarithm of the event time on covariates. The traditional AFT formulation assumes a linear relationship for the predictor, as shown in Eqs. (1) and (2). To overcome this restrictive linearity while maintaining interpretability, we introduce the KAN-AFT framework. In this model, the linear predictor $\mathbf{x}^\top \boldsymbol{\beta}$ in Eq. (2) is replaced by a nonlinear function $\eta(\mathbf{z})$, approximated using a Kolmogorov–Arnold Network (KAN):

$$\log T_i = \text{KAN}(\mathbf{z}_i) + \sigma \epsilon_i. \quad (3)$$

Here, \mathbf{z}_i represents the unaugmented input feature vector for the i -th individual, consisting of the p raw explanatory variables (covariates) used in the traditional AFT model (Eq. (1)). In the KAN architecture, this vector serves as the initial input layer. The output $\text{KAN}(\mathbf{z}_i)$ corresponds to the nonlinear predictor $\eta(\mathbf{z}_i)$ that generalizes the traditional linear form $\mathbf{x}_i^\top \boldsymbol{\beta}$. This structure preserves the intuitive time-scale interpretation of the AFT model while introducing the expressive nonlinearity and symbolic interpretability characteristic of KANs.

2.1 KAN Architecture for AFT Prediction

The Kolmogorov-Arnold Network (KAN) architecture (Liu et al., 2024) is inspired by the Kolmogorov-Arnold representation theorem (Braun and Griebel, 2009), which states that any continuous multivariate function can be represented as a finite composition and summation of univariate functions:

$$f(z_1, z_2, \dots, z_n) = \sum_{q=1}^{2n+1} \Phi_q \left(\sum_{p=1}^n \phi_{q,p}(z_p) \right).$$

KANs implement this principle by placing learnable univariate activation functions (ϕ) on the network edges, in contrast to Multi-Layer Perceptrons (MLPs) that use fixed non-linear activations at the nodes. This structure promotes both higher accuracy and inherent interpretability.

A KAN's structure is defined by its layer shape (n_0, n_1, \dots, n_L) , where n_l is the number of neurons in the l^{th} layer. The output of the $(l+1)^{\text{th}}$ layer, \mathbf{z}_{l+1} , is determined by summing the outputs of n_l learnable activation functions, $\phi_{l,j,i}$, applied to the previous layer's outputs, \mathbf{z}_l :

$$z_{l+1,j} = \sum_{i=1}^{n_l} \phi_{l,j,i}(z_{l,i}), \quad j = 1, 2, \dots, n_{l+1}.$$

These univariate activation functions, $\phi_{l,j,i}(\cdot)$, are typically parameterized by B-splines, allowing them to accurately approximate arbitrary smooth functions during training. In

matrix form:

$$\mathbf{z}_{l+1} = \underbrace{\begin{pmatrix} \phi_{l,1,1}(\cdot) & \phi_{l,1,2}(\cdot) & \cdots & \phi_{l,1,n_l}(\cdot) \\ \phi_{l,2,1}(\cdot) & \phi_{l,2,2}(\cdot) & \cdots & \phi_{l,2,n_l}(\cdot) \\ \vdots & \vdots & \ddots & \vdots \\ \phi_{l,n_{l+1},1}(\cdot) & \phi_{l,n_{l+1},2}(\cdot) & \cdots & \phi_{l,n_{l+1},n_l}(\cdot) \end{pmatrix}}_{\Phi_l} \mathbf{z}_l.$$

The final output of a general KAN with L layers is:

$$\text{KAN}(\mathbf{z}) = (\Phi_{L-1} \circ \Phi_{L-2} \circ \cdots \circ \Phi_0) \mathbf{z}.$$

For the KAN-AFT model, we use a minimal, shallow architecture $[\mathbf{n}_{\text{cov}}, \mathbf{1}]$, where the input layer has n_{cov} neurons (equal to the number of covariates) and the output layer consists of a single neuron. This reduces the KAN to a single-layer additive model, the components of which are detailed in Table 1:

$$\text{KAN}(\mathbf{z}) = \sum_{i=1}^{n_{\text{cov}}} \phi_{1,1,i}(z_i).$$

Table 1: Minimal KAN-AFT Architecture

Component	Description
Input Layer	Each of the p covariates forms the input neurons: $\mathbf{z}_i = (z_{i1}, \dots, z_{ip})^\top$
Activation Functions	Each input z_{ij} passes through a unique univariate learnable function $\phi_{1,1,j}(\cdot)$
Output Layer	Sum of all activation outputs: $\text{KAN}(\mathbf{z}_i) = \sum_{j=1}^p \phi_{1,1,j}(z_{ij})$

The activation functions $\phi(z)$ are parameterized as a combination of a base function $b(z)$ and a flexible B-spline expansion:

$$\phi(z) = w_b b(z) + w_s \sum_{j=0}^{G+k-1} c_j B_{j,k}(z),$$

where w_b, w_s are trainable weights, c_j are spline coefficients, and $B_{j,k}(z)$ are B-spline basis functions of degree k over G grid intervals. This structure ensures smooth, non-linear

approximation while maintaining interpretability.

2.2 Interpretability and Transparent Modeling

The KAN-AFT model's interpretability is secured through visualization and aggressive regularization, enabling the potential discovery of the underlying symbolic relationship between covariates and log-survival time.

To promote model simplicity and prevent overfitting, a regularization term, L_R , is incorporated into the overall loss function L_{Total} . This term encourages sparsity in both the activation functions (Φ) and their defining spline coefficients (\mathbf{C}):

$$L_{Total} = L_{survival} + L_R$$

$$L_R = \sum_{l=0}^{L-1} |\Phi_l|_1 + \lambda_1 \sum_{l=0}^{L-1} S(\Phi_l) + \lambda_2 \sum_{l=0}^{L-1} |\mathbf{C}_l|_1.$$

- $|\Phi_l|_1$: L_1 -norm regularization on the magnitude of activation functions, which forces negligible connections to zero, facilitating pruning.
- $S(\Phi_l)$: Entropy regularization, defined as $S(\Phi) \equiv - \sum_i \sum_j \frac{|\phi_{i,j}|_1}{|\Phi|_1} \log \left(\frac{|\phi_{i,j}|_1}{|\Phi|_1} \right)$, which promotes modularity and feature selection.
- $|\mathbf{C}_l|_1$: L_1 -norm on the spline coefficients, promoting simpler, less oscillatory function shapes.

Following training and pruning, the smooth B-spline functions $\phi(z)$ are subjected to a final stage of symbolic discovery (or symbolic regression). This process converts the high-performance, non-linear functions learned by the KAN into a final, explicit, and human-readable symbolic equation. This symbolic output directly reveals the exact non-linear influence of the covariate on the logarithm of the failure time, $\log T$:

- If the model discovers $\phi(z) \approx \exp(z)$, the covariate's effect is found to be exponential and accelerating.
- If the model discovers $\phi(z) \approx \sin(z^2)$, the covariate's effect is found to be periodic and oscillating.

This transformation (e.g., $\phi(z) \approx \exp(z)$ or $\phi(z) \approx \sin(z^2)$) yields significant scientific insight by converting a flexible B-spline into a transparent, verifiable mathematical formula.

2.3 Censoring Mechanisms

The AFT model requires estimation of the time-to-event X , but this variable is often unobserved due to right censoring. Let C denote the censoring time. For n individuals, the observed data consists of the tuple $(T_i, \delta_i, \mathbf{z}_i)$, where $T_i = \min(X_i, C_i)$ is the observed time, $\delta_i = I(X_i \leq C_i)$ is the censoring indicator (1 if the event is observed, 0 otherwise), and \mathbf{z}_i are the covariates. We assume X and C are conditionally independent given \mathbf{z} .

The objective remains to estimate the KAN predictor $\Phi(\mathbf{z}_i) = \text{KAN}(\mathbf{z}_i)$ in the model $\log T_i = \Phi(\mathbf{z}_i) + \sigma \epsilon_i$. Since the AFT model is a regression framework, we adapt three established methods from the DeepAFT literature (Norman et al., 2024) to handle right-censoring. The final predicted survival time \hat{T}_i is obtained by exponentiating the KAN's output $\hat{\Phi}(\mathbf{z}_i)$:

$$\hat{T}_i = \exp(\hat{\Phi}(\mathbf{z}_i)).$$

2.3.1 KAN-AFT-BuckleyJames (Iterative Imputation)

The Buckley-James method (Buckley and James, 1979) is a powerful approach for handling censored data that essentially adapts standard regression (like Ordinary Least Squares) to the survival setting. Unlike methods that assume a specific distribution for the error term, this method is semi-parametric, meaning it makes no such restrictive distributional assumptions, giving it greater flexibility.

The core idea of KAN-AFT-BuckleyJames is iterative imputation. For every observation where we only know the time-to-event was censored (the event hadn't happened yet), the method estimates (imputes) what the actual, full time-to-event would have been. It does this not by guessing the absolute time, but by focusing on the residuals (the error between the current model prediction and the observed time).

1. Initialization: Set an initial estimate for the KAN predictor, $\hat{\Phi}^{(0)}(\mathbf{z}_i) = 0$.
2. Residual Calculation: At iteration k , the survival data are transformed into residual

times, $\gamma_i^{(k-1)}$, based on the previous KAN estimate:

$$\gamma_i^{(k-1)} = T_i / \exp \left(\hat{\Phi}^{(k-1)}(\mathbf{z}_i) \right).$$

3. Imputation: The unobserved residual times for censored observations ($\delta_i = 0$) are imputed by calculating the conditional expectation of the residuals, $E(\gamma | \gamma > \gamma_i^{(k-1)})$, using the non-parametric Kaplan-Meier estimator applied to the residual distribution. This yields the imputed residual $\gamma_i^{*(k-1)}$.
4. Target Update: A new imputed log-time target, $Y_i^{*(k)}$, is constructed:

$$Y_i^{*(k)} = \hat{\Phi}^{(k-1)}(\mathbf{z}_i) + \log \gamma_i^{*(k-1)}.$$

5. KAN Training: The KAN model is trained on the imputed data $(\mathbf{z}_i, Y_i^{*(k)})$ using the standard, unweighted Mean Squared Error (MSE) loss:

$$L_{MSE}^{(k)} = \frac{1}{n} \sum_{i=1}^n \left(Y_i^{*(k)} - \text{KAN}(\mathbf{z}_i) \right)^2.$$

6. Convergence: The process is repeated until convergence, where the change in the KAN estimate, $|\hat{\Phi}^{(k)} - \hat{\Phi}^{(k-1)}|$, falls below a specified threshold.

Algorithm 1 presents the pseudo-code for this mechanism, which, due to its iterative nature, follows a defined sequence of initialization, imputation, KAN training, and convergence steps.

2.3.2 KAN-AFT-IPCW (Inverse Probability of Censoring Weights)

KAN-AFT-IPCW approach integrates the KAN architecture with the Inverse Probability of Censoring Weights (IPCW) method (Robins and Rotnitzky, 1992) to handle incomplete data, which is common in survival analysis. The core idea is to correct the bias introduced when we can only observe the event time for some individuals (uncensored data) and must exclude or downplay others (censored data). This method is appealing because it is non-iterative.

Instead of trying to guess the full time-to-event for censored observations, KAN-AFT-

Algorithm 1: Iterative KAN-AFT Buckley–James Censoring Psuedo-code

Data: Observed data $\mathcal{D} = \{(T_i, \delta_i, \mathbf{z}_i)\}_{i=1}^n$, Max Iterations K , Tolerance τ

Result: Trained KAN predictor $\hat{\Phi}(\mathbf{z})$

Initialization: Set $\hat{\Phi}^{(0)}(\mathbf{z}_i) = 0$ for all i . Set $k \leftarrow 1$;

while $k \leq K$ **and** $\frac{1}{n} \sum_{i=1}^n |\hat{\Phi}^{(k)}(\mathbf{z}_i) - \hat{\Phi}^{(k-1)}(\mathbf{z}_i)| \geq \tau$ **do**

for $i = 1$ **to** n **do**

| Compute residual: $\gamma_i^{(k-1)} \leftarrow T_i / \exp(\hat{\Phi}^{(k-1)}(\mathbf{z}_i))$;

end

Estimate residual survival function $\hat{S}_\gamma(\cdot)$ using Kaplan-Meier on $\{\gamma_i^{(k-1)}\}$;

for $i = 1$ **to** n **do**

if $\delta_i = 1$, (Uncensored), **then**

| Imputed residual: $\gamma_i^{*(k-1)} \leftarrow \gamma_i^{(k-1)}$;

end

else

$\delta_i = 0$, (Censored), Calculate conditional expectation:

$E \leftarrow E(\gamma | \gamma > \gamma_i^{(k-1)})$;

| Imputed residual: $\gamma_i^{*(k-1)} \leftarrow E$;

end

| Update imputed target: $Y_i^{*(k)} \leftarrow \hat{\Phi}^{(k-1)}(\mathbf{z}_i) + \log \gamma_i^{*(k-1)}$;

end

Train KAN: Find $\hat{\Phi}^{(k)}$ by minimizing standard MSE loss, $L_{MSE}^{(k)}$;

$L_{MSE}^{(k)} = \frac{1}{n} \sum_{i=1}^n (Y_i^{*(k)} - \text{KAN}(\mathbf{z}_i))^2$ $k \leftarrow k + 1$;

end

return $\hat{\Phi}^{(k-1)}$ (the converged predictor);

IPCW trains the KAN directly on the observed log-times (Y_i) but uses a modified loss function to give more importance (a weight, w_i) to observations that were less likely to be censored. This ensures that the model learns the true underlying relationship primarily from the reliable, uncensored data, effectively removing the bias caused by censoring.

1. Weight Calculation: The Inverse Probability of Censoring Weights (IPCW) w_i is calculated for each observation, where $\hat{G}(T_i)$ is the Kaplan-Meier estimator for the censoring distribution C :

$$w_i = \frac{\delta_i}{\hat{G}(T_i)}.$$

2. Adjusted Loss: The KAN is trained directly on the observed log-times, Y_i , using the Adjusted Mean Squared Error (AMSE) loss, which effectively ignores censored

observations ($\delta_i = 0 \implies w_i = 0$):

$$L_{AMSE} = \frac{1}{n} \sum_{i=1}^n w_i (Y_i - \text{KAN}(\mathbf{z}_i))^2.$$

2.3.3 KAN-AFT-Transform (Transformation Method)

KAN-AFT-Transform method adopts the transformation approach proposed by Fan and Gijbels (Fan et al., 1997), which provides an elegant solution to the challenges of censored data by redefining the time variable. The main idea is to transform the observed, possibly censored time-to-event data (T_i) into a new variable (T_i^*) that follows a standard probability distribution.

Once the data are transformed, the survival analysis problem can be treated as a standard regression task. This enables the KAN-AFT model to be trained efficiently using the Mean Squared Error (MSE) loss, avoiding the need for iterative imputation (as in KAN-AFT-BuckleyJames) or dynamic weighting (as in KAN-AFT-IPCW).

1. Transformation: The observed time T_i is transformed into an adjusted time T_i^* :

$$T_i^* = \phi_1(T_i) \cdot \delta_i + \phi_2(T_i) \cdot (1 - \delta_i),$$

where $\phi_1(T)$ and $\phi_2(T)$ are defined as:

$$\phi_1(T) = (1 + \alpha) \int_0^T \frac{du}{\hat{G}(u)} - \alpha \frac{T}{\hat{G}(T)}$$

and

$$\phi_2(T) = (1 + \alpha) \int_0^T \frac{du}{\hat{G}(u)}.$$

Here, $\hat{G}(u)$ is the Kaplan-Meier estimator for the censoring distribution. The tuning parameter α is determined such that $T_i^* \geq 0$ for all i , and is calculated as:

$$\alpha = \min_{i: \delta_i=1} \left(\frac{\int_0^{T_i} \hat{G}(u)^{-1} du - T_i}{T_i \hat{G}(T_i)^{-1} - \int_0^{T_i} \hat{G}(u)^{-1} du} \right).$$

2. KAN Training: The KAN is trained on the transformed log-times, $\log T_i^*$, using the

standard MSE loss which aims to fit the predictor defined in Eq. (3):

$$L_{MSE} = \frac{1}{n} \sum_{i=1}^n (\log T_i^* - \text{KAN}(\mathbf{z}_i))^2.$$

Building on the KAN-AFT framework and censoring-handling strategies, we next evaluate the model's performance. Section 3 assesses KAN-AFT using synthetic datasets as well as real-world datasets to demonstrate its predictive accuracy and practical applicability.

3. Simulation Study

The proposed KAN-AFT model is evaluated using both simulated synthetic data and real-world datasets. The synthetic datasets are generated to progressively test the model's capacity: one with strictly linear covariate effects, and one with non-linear covariate effects.

3.1 Linear synthetic data

The linear simulated data consists of 1000 observations with observed time, event status and three covariate features. The covariates (\mathbf{z}) are randomly generated from standard normal distribution. The log times are the linear combination of features with random error and T' is the simulated time. We generate censored observations (\mathbf{C}) from exponential distribution with parameter $\lambda = 10$ and obtain observed time T as the minimum of simulated time and simulated censored observations, $T = \min(T', C)$. We simulate random error in Eq. (2) from normal distribution. The true AFT survival model is

$$\log T = 0.5z_1 - 0.3z_2 + z_3 + \epsilon.$$

The KAN-AFT model network is given in Figure 1 and identified the linear relationship by symbolic regression, the obtained formula is given as:

$$\log T = 0.5113z_1 - 0.3081z_2 + 0.9483z_3 - 0.0556 \quad (\text{Buckley James})$$

$$\log T = 0.4043z_1 - 0.2086z_2 + 0.7463z_3 - 0.0842 \quad (\text{IPCW})$$

$$\log T = 0.4556z_1 - 0.2529z_2 + 0.8480z_3 - 0.0208 \quad (\text{Transform})$$

Figure 1 illustrates the model’s performance in scenarios where the relationship between the covariates and survival time is linear. By applying the KAN-AFT architecture to synthetic data, the network diagrams for the Buckley-James, IPCW, and Transform methods show that the activation functions on the edges converge into straight lines. This visual simplification demonstrates how the Kolmogorov-Arnold Network identifies linear patterns and performs symbolic regression to produce a transparent mathematical equation. This allows the model to achieve the clarity of traditional parametric models while retaining the flexibility of a neural network.

The performance of KAN-AFT model is compared with parametric AFT model and DeepAFT model using C-index and MSE as the evaluation metrics and the results are shown in Table 2. KAN-AFT model outperforms DeepAFT model and gets the C-index which is close to parametric AFT models. The MSE is smaller for KAN-AFT compared to other models and it ensures that the observed time and predicted time is similar for the proposed model.

Table 2: Performance Comparison of AFT, DeepAFT, and KAN-AFT Models on the Linear Synthetic Data. Metrics include Concordance Index (C-index) and Mean Squared Error (MSE) on both the training and testing sets.

Model	C-index		MSE	
	Train	Test	Train	Test
AFT-Weibull	0.8684	0.8724	1.1223	0.9754
AFT-Log-normal	0.8686	0.8741	1.1389	0.8755
AFT-Log-logistic	0.8684	0.8741	1.1376	0.8724
DeepAFT-BuckleyJames	0.8241	0.7835	4.3393	3.2239
DeepAFT-IPCW	0.8070	0.8018	2.2439	1.1326
DeepAFT-Transform	0.8158	0.8107	3.9888	2.2821
KAN-AFT-BuckleyJames	0.8690	0.8750	0.2500	0.2879
KAN-AFT-IPCW	0.8641	0.8691	0.3333	0.3554
KAN-AFT-Transform	0.8675	0.8727	0.2616	0.3072

3.2 Non-linear data

The non-linear simulated data consists 1000 observations with observed time, event status and three covariate features. The covariates (\mathbf{z}) are randomly generated from standard normal distribution. The log times are the linear combination of features with random error

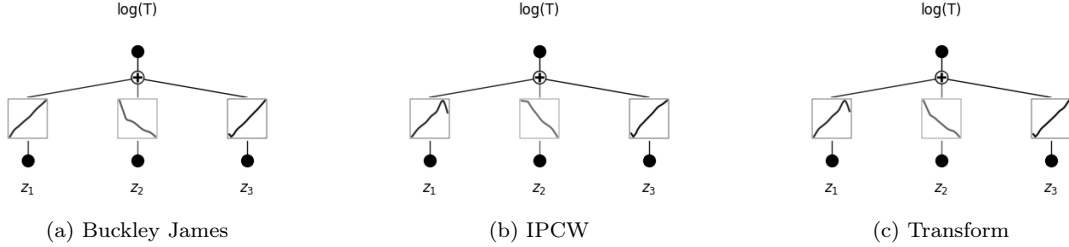


Figure 1: KAN - AFT network for linear synthetic data.

and denote T' as the simulated time. We generate censored observations (C) from exponential distribution with parameter $\lambda = 10$ and obtain observed time T as the minimum of simulated time and simulated censored observations, $T = \min(T', C)$. We simulate random error in Eq. (2) from normal distribution. The true AFT survival model is

$$\log T = 0.5z_1^2 + 0.3 \exp(z_2) + 0.8 \sin(z_3) + \epsilon.$$

The non-linear covariate effects are correctly identified with three KAN-AFT methods and the corresponding networks are given in Figure 2. The performance comparison of different models on non linear synthetic data is given in Table 3. From the results, it is evident that the KAN-AFT model shows better C-index and smaller MSE than other models. Since KAN-AFT shows higher C-index than DeepAFT, the model is more efficient to deal with non-linear relationship.

Figure 2 highlights the primary strength of the KAN-AFT model in capturing complex, non-linear relationships that often challenge standard survival models. In this case, the underlying data involves quadratic, exponential, and sine functions. The figure displays how the learned activation functions on the network edges take on distinct shapes that directly correspond to these mathematical operations. By visualizing these "edge" functions, the model moves beyond traditional "black-box" predictions. It provides a clear view of the specific non-linear effects, such as a squared term or a periodic cycle, making the research findings more interpretable and scientifically robust for clinical applications.

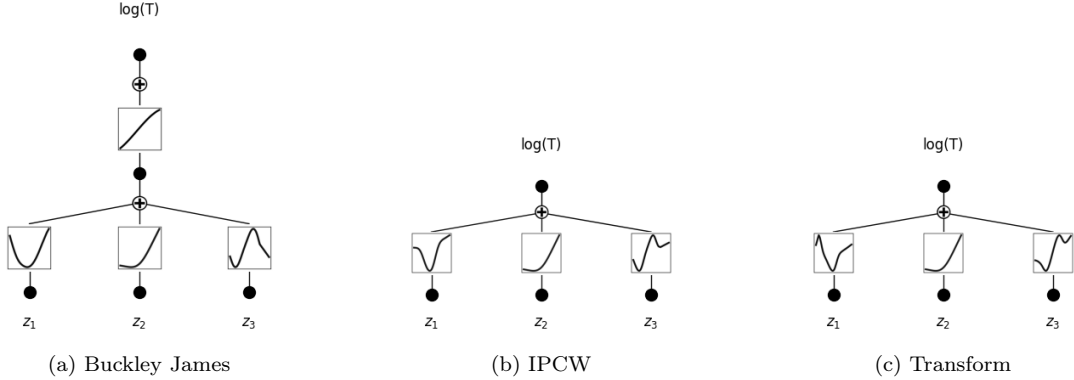


Figure 2: KAN - AFT network for non linear synthetic data.

Table 3: Performance Comparison of AFT, DeepAFT, and KAN-AFT Models on the Non Linear Synthetic Data. Metrics include Concordance Index (C-index) and Mean Squared Error (MSE) on both the training and testing sets.

Model	C-index		MSE	
	Train	Test	Train	Test
AFT-Weibull	0.7387	0.7251	6.9738	7.2768
AFT-Log-normal	0.7415	0.7293	6.4513	6.7199
AFT-Log-logistic	0.7432	0.7328	6.4807	6.7034
DeepAFT-BuckleyJames	0.7477	0.7228	6.2107	6.4105
DeepAFT-IPCW	0.7892	0.7797	4.0080	4.3852
DeepAFT-Transform	0.7691	0.7560	5.8764	6.1042
KAN-AFT-BuckleyJames	0.8505	0.8419	0.2810	0.2995
KAN-AFT-IPCW	0.8317	0.8281	0.4354	0.4087
KAN-AFT-Transform	0.8403	0.8365	0.3007	0.2853

4. Real Applications

The model's performance is further assessed using PBC, GBSG, Veteran, and Heart failure data as real data sets and compared the performance of this model with parametric AFT and DeepAFT.

4.1 Primary Biliary Cholangitis Data (PBC)

Mayo Clinic Primary Biliary Cholangitis Data (PBC) (Therneau and Grambsch, 2000) is used for demonstrating KAN-AFT in real world scenario. This dataset contains a total of 418 PBC patients in which 232 patients are censored or lost to follow up. The important

covariates are age (years), albumin: serum albumin (g/dl), alk.phos: alkaline phosphatase (U/liter), ast: aspartate aminotransferase (U/ml), bili: serum bilirubin (mg/dl), chol: serum cholesterol (mg/dl), copper: urine copper (ug/day), platelet: platelet count, protime: standardised blood clotting time and trig: triglycerides (mg/dl).

We perform Schoenfeld residuals test (Grambsch and Therneau, 1994) for each covariate and a global test for the model as a whole to determine violation of the proportional hazards assumption. Chi square test statistic and the corresponding p-values are shown in Table 4. The p-values for some covariates, bili, chol, trig, platelet, and protime are less than 0.05 indicates the failure of PH assumption. The global test also confirms that the PH assumption of the overall Cox model is not valid.

Since the violation of PH assumption, AFT model can be preferred over traditional Cox model. We fit KAN-AFT to the PBC data and the performance of this model is compared with AFT and DeepAFT model obtained the result as given in Table 5. From the result,

Table 4: Results of proportional hazards assumption validity check for PBC data (p value of < 0.05 indicates the violation of PH assumption)

Covariates	χ^2 -value	p-value
age	2.52	0.1122
bili	10.50	0.0012
chol	9.69	0.0019
albumin	1.57	0.2095
copper	0.42	0.5171
alk.phos	1.53	0.2160
ast	1.35	0.2450
trig	5.98	0.0145
platelet	3.94	0.0472
protime	4.51	0.0338
Global	26.90	0.0027

KAN-AFT Buckley James model obtains the best C-index and other KAN-AFT models outperforms DeepAFT model and achieve comparable C-index to parametric AFT models. Since the distribution assumption of parametric AFT is not assumed, KAN-AFT can be considered as a better model than parametric AFT.

Table 5: Performance Comparison of C index in AFT, DeepAFT, and KAN-AFT Models on the PBC dataset on both the training and testing sets.

Model	C-index	
	Train	Test
AFT-Weibull	0.8058	0.7958
AFT-Log-normal	0.8046	0.7993
AFT-Log-logistic	0.8045	0.7958
DeepAFT-BuckleyJames	0.7504	0.7729
DeepAFT-IPCW	0.6595	0.6474
DeepAFT-Transform	0.7053	0.6955
KAN-AFT-BuckleyJames	0.8407	0.7718
KAN-AFT-IPCW	0.7773	0.7947
KAN-AFT-Transform	0.8020	0.7787

4.2 German Breast Cancer Study Group (GBSG) Data

The GBSG data set contains patient records from a 1984-1989 trial conducted by the German Breast Cancer Study Group (GBSG) (Royston and Altman, 2013) of 720 patients with node positive breast cancer and it retains the 686 patients with 387 censored observations with complete data for the prognostic variables. The main prognostic variables (covariates) in the data are grade:tumor grade, nodes:number of positive lymph nodes, pgr:progesterone receptors (fmol/l), and er:estrogen receptors (fmol/l). We fit KAN-AFT

Table 6: Performance Comparison of C-index in AFT, DeepAFT, and KAN-AFT Models on the GBSG dataset on both the training and testing sets.

Model	C-index	
	Train	Test
AFT-Weibull	0.6756	0.7088
AFT-Log-normal	0.6759	0.6999
AFT-Log-logistic	0.6762	0.7004
DeepAFT-BuckleyJames	0.5427	0.5200
DeepAFT-IPCW	0.5446	0.5375
DeepAFT-Transform	0.5532	0.5378
KAN-AFT-BuckleyJames	0.7066	0.7099
KAN-AFT-IPCW	0.6447	0.6548
KAN-AFT-Transform	0.6798	0.7058

model for the GBSG data and compared train and test C-index with parametric AFT and DeepAFT. The The performance comparison is presented in Table 6. KAN-AFT model using Buckley James and transform method achieve higher C-index than parametric AFT and DeepAFT models in both training and test sets. Here the proportional hazard assumption of the Cox model is valid but KAN-AFT is also suitable for the data since it does not consider any assumptions and deals with complex relationships.

4.3 Veteran Data

Veteran data (Kalbfleisch and Prentice, 2002) is a randomised trial of two treatment regimens for lung cancer. The data consists of observations from 137 patients in which 9 patients are censored and lost to follow up. The covariates include karno: Karnofsky performance score (100=good), diagtime: months from diagnosis to randomisation, and age: in years.

The PH assumption is validated for each covariates and globally for the data, the obtained test statistic and p-values are summarized in Table 7. The covariate karno fails to satisfy the PH assumption since the p-value is less than 0.05. The overall global test also suggests the violation of PH assumption of Cox model. The failure of PH assumption suggests to fit AFT

Table 7: Results of proportional hazards assumption validity check for veteran data (p value of < 0.05 indicates the violation of PH assumption)

Covariates	χ^2 -value	p-value
karno	13.09572	0.00030
diagtime	0.00762	0.93042
age	2.13545	0.14393
Global	17.80455	0.00048

model for the Veteran data. We fit KAN-AFT model to include non-linear relationships and compare with parametric AFT and DeepAFT. The results are presented in Table 8. The three KAN-AFT model outperforms DeepAFT models except DeepAFT IPCW and achieves higher C-index than parametric AFT in training set. In test set, the C-index for KAN-AFT is very close to parametric AFT models. Since the distribution assumption is not assumed, KAN-AFT is more efficient than AFT regression models.

Table 8: Performance Comparison of C index in AFT, DeepAFT, and KAN-AFT Models on the Veteran dataset on both the training and testing sets.

Model	C-index	
	Train	Test
AFT-Weibull	0.7064	0.7285
AFT-Log-normal	0.7113	0.7064
AFT-Log-logistic	0.7111	0.7091
DeepAFT-BuckleyJames	0.7124	0.6884
DeepAFT-IPCW	0.7179	0.6911
DeepAFT-Transform	NA	NA
KAN-AFT-BuckleyJames	0.7131	0.7202
KAN-AFT-IPCW	0.7126	0.7008
KAN-AFT-Transform	0.7136	0.7036

4.4 Heart Failure Clinical Record Data

The Heart failure clinical record data (Chicco and Jurman, 2020) contains the medical records of 299 patients who had heart failure, collected during their follow-up period, where each patient profile has 13 clinical features. The important features are age:age of the patient, creatinine phosphokinase:level of the CPK enzyme in the blood (mcg/L), ejection fraction : percentage of blood leaving the heart at each contraction, platelets : platelets in the blood (kiloplatelets/mL), serum creatinine:level of serum creatinine in the blood (mg/dL) and serum sodium: level of serum sodium in the blood (mEq/L). We fit three KAN-AFT models with the features for the Heart failure data. The comparison of performance of KAN-AFT model to parametric AFT and DeepAFT models is provided in Table 9. The three KAN-AFT models outperform DeepAFT in C-index for both training and test data. KAN-AFT with Buckley James and IPCW methods achieve higher C-index than parametric AFT models in training data but parametric AFT outperforms KAN-AFT in test C-index. The KAN-AFT model and parametric AFT models perform well for the Heart failure data even though the PH assumption of Cox model is valid.

5. Discussions

This study introduces the KAN-AFT model as a flexible and interpretable alternative for survival analysis in settings where classical modeling assumptions are restrictive or violated.

Table 9: Performance Comparison of C index in AFT, DeepAFT, and KAN-AFT Models on the Heart failure dataset on both the training and testing sets.

Model	C-index	
	Train	Test
AFT-Weibull	0.7149	0.7593
AFT-Log-normal	0.7145	0.7593
AFT-Log-logistic	0.7155	0.7581
DeepAFT-BuckleyJames	0.6800	0.7182
DeepAFT-IPCW	0.5339	0.5262
DeepAFT-Transform	0.5403	0.5461
KAN-AFT-BuckleyJames	0.7504	0.6796
KAN-AFT-IPCW	0.7210	0.7157
KAN-AFT-Transform	0.6484	0.6895

By integrating the accelerated failure time (AFT) framework with Kolmogorov–Arnold Networks, the proposed approach directly models survival time while allowing covariate effects to be nonlinear, heterogeneous, and data-adaptive. This combination is particularly relevant for modern biomedical and reliability datasets, which often exhibit non-proportional hazards, complex covariate interactions, and moderate sample sizes with substantial censoring.

The simulation studies demonstrate that KAN-AFT performs robustly across both linear and nonlinear data-generating mechanisms. When covariate effects are linear, KAN-AFT achieves performance comparable to classical linear AFT models, indicating no loss of efficiency due to model flexibility. In nonlinear scenarios, however, KAN-AFT clearly outperforms linear and parametric AFT counterparts, highlighting its ability to recover complex functional relationships without requiring prior specification of their form.

Real-data analyses further illustrate the practical advantages of KAN-AFT. In datasets where the proportional hazards assumption is violated, such as the Primary Biliary Cholangitis (PBC) data, Cox-type models may yield unstable or misleading interpretations. While parametric AFT models offer an improvement by focusing on survival time, their performance depends critically on correct distributional assumptions, which are rarely verifiable in practice. KAN-AFT alleviates this limitation by learning covariate effects directly from the data, achieving predictive performance comparable to or better than parametric AFT

models without relying on strict parametric forms.

A key strength of the proposed approach lies in its interpretability. Unlike black-box deep survival models, KAN-AFT yields explicit symbolic representations of covariate effects on log-survival time. These expressions allow researchers and practitioners to examine the shape, direction, and relative importance of covariate effects, facilitating scientific insight and clinical validation. This interpretability is particularly important in medical and reliability applications, where transparency and trust are essential for model adoption and decision-making.

From a methodological perspective, KAN-AFT bridges the gap between classical survival models and modern machine learning approaches. It preserves the intuitive time-acceleration interpretation of AFT models while incorporating the flexibility of nonlinear function learning. This balance enables KAN-AFT to serve as a practical tool for applied analysts who require both predictive accuracy and explainability, especially in complex survival settings where traditional assumptions fail.

Despite its advantages, the proposed framework has certain limitations. As with other flexible models, careful regularization and tuning are required to avoid overfitting, particularly in small samples. Additionally, while symbolic representations enhance interpretability, their complexity may increase with the number of covariates and network depth. Future work could focus on extending KAN-AFT to handle time-dependent covariates, competing risks, and high-dimensional settings, as well as developing formal inference procedures for the learned functional effects.

In conclusion, KAN-AFT provides a robust, interpretable, and assumption-light framework for survival analysis. By combining the strengths of AFT models and Kolmogorov–Arnold Networks, it offers a compelling alternative to both classical parametric methods and black-box deep learning approaches. Strong empirical performance and practical interpretability collectively support the use of KAN-AFT as a valuable addition to the survival analysis toolkit.

References

Braun, J., Griebel, M., 2009. On a constructive proof of kolmogorov's superposition theorem. *Constructive approximation* 30, 653–675.

Buckley, J., James, I., 1979. Linear regression with censored data. *Biometrika* 66, 429–436.

Chen, Y., Jia, Z., Mercola, D., Xie, X., 2013. A gradient boosting algorithm for survival analysis via direct optimization of concordance index. *Computational and mathematical methods in medicine* 2013, 873595.

Chicco, D., Jurman, G., 2020. Machine learning can predict survival of patients with heart failure from serum creatinine and ejection fraction alone. *BMC medical informatics and decision making* 20, 16.

Cox, D.R., 1972. Regression models and life-tables. *Journal of the Royal Statistical Society: Series B (Methodological)* 34, 187–202.

Fan, J., Gijbels, I., 1994. Censored regression: local linear approximations and their applications. *Journal of the American Statistical Association* 89, 560–570.

Fan, J., Gijbels, I., King, M., 1997. Local likelihood and local partial likelihood in hazard regression. *The Annals of Statistics* 25, 1661–1690.

Faraggi, D., Simon, R., 1995. A neural network model for survival data. *Statistics in medicine* 14, 73–82.

Grambsch, P.M., Therneau, T.M., 1994. Proportional hazards tests and diagnostics based on weighted residuals. *Biometrika* 81, 515–526.

Hutton, J.L., Monaghan, P., 2002. Choice of parametric accelerated life and proportional hazards models for survival data: asymptotic results. *Lifetime data analysis* 8, 375–393.

Ishwaran, H., Kogular, U.B., Blackstone, E.H., Lauer, M.S., 2008. Random survival forests. *The Annals of Applied Statistics* 2, 841–860.

Kalbfleisch, J.D., Prentice, R.L., 2002. The statistical analysis of failure time data. John Wiley & Sons.

Katzman, J.L., Shaham, U., Cloninger, A., Bates, J., Jiang, T., Kluger, Y., 2018. Deepsurv: personalized treatment recommender system using a cox proportional hazards deep neural network. *BMC medical research methodology* 18, 24.

Klein, J.P., Moeschberger, M.L., 2003. Survival Analysis: Techniques for Censored and Truncated Data. Springer.

Knottenbelt, W., McGough, W., Wray, R., Zhang, W.Z., Liu, J., Machado, I.P., Gao, Z., Crispin-Ortuzar, M., 2025. Coxkan: Kolmogorov-arnold networks for interpretable, high-performance survival analysis. *Bioinformatics* 41, btaf413.

Lee, C., Zame, W., Yoon, J., Van Der Schaar, M., 2018. Deephit: A deep learning approach to survival analysis with competing risks, in: *Proceedings of the AAAI conference on artificial intelligence*.

Lee, E.T., Wang, J., 2003. Statistical methods for survival data analysis. volume 476. John Wiley & Sons.

Liu, Z., Wang, Y., Vaidya, S., Ruehle, F., Halverson, J., Soljačić, M., Hou, T.Y., Tegmark, M., 2024. Kan: Kolmogorov-arnold networks. *arXiv preprint arXiv:2404.19756* .

Norman, P.A., Li, W., Jiang, W., Chen, B.E., 2024. deepaft: A nonlinear accelerated failure time model with artificial neural network. *Statistics in Medicine* 43, 3689–3701.

Robins, J.M., Rotnitzky, A., 1992. Recovery of information and adjustment for dependent censoring using surrogate markers, in: *AIDS epidemiology: methodological issues*. Springer, pp. 297–331.

Royston, P., Altman, D.G., 2013. External validation of a cox prognostic model: principles and methods. *BMC medical research methodology* 13, 33.

Somvanshi, S., Javed, S.A., Islam, M.M., Pandit, D., Das, S., 2025. A survey on kolmogorov-arnold network. *ACM Computing Surveys* 58, 1–35.

Swindell, W.R., 2009. Accelerated failure time models provide a useful statistical framework for aging research. *Experimental gerontology* 44, 190–200.

Therneau, T.M., Grambsch, P.M., 2000. The cox model, in: *Modeling survival data: extending the Cox model*. Springer, pp. 39–77.

Wang, P., Li, Y., Reddy, C.K., 2019. Machine learning for survival analysis: A survey. *ACM Computing Surveys (CSUR)* 51, 1–36.

Wei, L.J., 1992. The accelerated failure time model: a useful alternative to the cox regression model in survival analysis. *Statistics in medicine* 11, 1871–1879.

Xu, L., Guo, C., 2023. Coxnam: An interpretable deep survival analysis model. *Expert Systems with Applications* 227, 120218.